

Article citation info:

Białostocka AM, Klekotka M, Klekotka U, Kalska-Szostko B. Tribological properties of the FeNi alloys electrodeposited with and without external magnetic field assistance. *Eksploracja i Niezawodność – Maintenance and Reliability* 2022; 24 (4): 687–694, <http://doi.org/10.17531/ein.2022.4.9>

Tribological properties of the FeNi alloys electrodeposited with and without external magnetic field assistance

Indexed by:



Anna Maria Białostocka^a, Marcin Klekotka^b, Urszula Klekotka^c, Beata Kalska-Szostko^c

^aBiałystok University of Technology, Faculty of Electrical Engineering, Department of Electrotechnics, Power Electronics and Electrical Power Engineering, ul. Wiejska 45D, 15-351 Białystok, Poland

^bBiałystok University of Technology, Faculty of Mechanical Engineering, Institute of Biomedical Engineering, ul. Wiejska 45C, 15-351 Białystok, Poland

^cUniversity of Białystok, Faculty of Chemistry, Department of Physical Chemistry, ul. Ciołkowskiego 1K, 15-245 Białystok, Poland

Highlights

- An effective method of the FeNi electrodeposition on two substrates is presented.
- The tribological properties of magneto-electrodeposited FeNi coatings were determined.
- The FeNi layers properties are influenced by an external magnetic field.
- The FeNi surface morphology is related to the Fe content and the type of the substrate.

Abstract

The hereby work presents the tribological properties of the iron-nickel alloys and their dependence on the microstructure and thickness of the probes as well as the presence of an external magnetic field during the synthesis. Coatings were electroplated on the brass and copper metallic substrates using galvanostatic deposition in the same electrochemical bath condition (Fe and Ni sulfates) and the electric current density. The surface morphology of the films was observed by Scanning Electron Microscopy. The average composition of all FeNi coatings was measured using Energy Dispersive X-ray Spectroscopy. Tribo-mechanical properties such as microhardness, roughness, and friction coefficient were determined in the obtained structures. The morphology and tribological properties of the FeNi coatings clearly depend on both the substrate (Cu, CuZn) itself and the presence of an external magnetic field (EMF) applied during the deposition process.

Keywords

This is an open access article under the CC BY license (<https://creativecommons.org/licenses/by/4.0/>)

electrodeposition, magnetic fields, Cu and CuZn substrate, FeNi coatings, microhardness, roughness, friction, wear.

1. Introduction

There is a wide range of processes that can alter the morphology and properties of metals. This is one of the advantages of metals because processing itself may be the source of defects in the final product. Continuous monitoring leads to better materials synthesis methods, capable to achieve accurate control of the structure and atomic configuration of the crystals at the nanoscale [24, 31, 37]. The electrodeposition is successfully used during the production of the multi layers (ML) coatings because of its simplicity, low manufacturing cost, and versatility. Nowadays, this process is further developed to predict and tailor the functional properties as the result of a quantitative description of fundamental phenomena at the atomic scale. Electrodeposited metals and alloys characterize enhanced micromechanical properties in comparison to cast metals and alloys [9, 13, 32]. The variation of the parameters such as electrolyte composition, bath pH, temperature, agitation (the physiochemical conditions), current density, potential (the electric conditions), and magnetic field can alter the composition

and microstructure of the deposited layers. This, in turn, affects the tribological properties of the layers, which are extremely important for their subsequent use in many areas of industry and economy and is essential [5]. A good example is the increasing significant demands to control friction losses and decrease the wear of machine components. Process of the tribo-mechanical and physical properties tailoring, such as wear resistance, high-temperature corrosion protection, oxidation resistance, and lubrication properties of a metallic coating, allows for achieving many different application requirements [12, 13]. Pure metal (Ni or Fe) exhibits different specific properties than the alloy (FeNi) received after the manufacturing process [13]. Differences in their percentage composition result in potential changes in later applications. The FeNi coatings could be used for example as high-performance transformers cores, read/writer magnetic shield materials, magnetic actuators, composites molds/tooling, etc. [1, 2]. Mentioned ML coatings are investigated by many researchers and have attracted attention due to their mechanical, electric, and magnetic properties [8,

(*) Corresponding author.

E-mail addresses: A.M. Białostocka (ORCID: 0000-0002-7684-2357): a.bialostocka@pb.edu.pl, M. Klekotka (ORCID: 0000-0002-9751-2939): m.klekotka@pb.edu.pl, U. Klekotka (ORCID: 0000-0002-1594-5889): u.wykowska@uwb.edu.pl, B. Kalska-Szostko (ORCID: 0000-0002-6353-243X): kalska@uwb.edu.pl

13, 28, 32]. Alloying of the substrate surface is often implemented for improving the coating performance, especially to increase the efficiency of mechanical systems or reduce friction losses using advanced materials and surface technologies. Additionally could be applied low-quality substrate (nonmetallic or metallic material) and its cover may satisfy the user which reduces the cost of application. Direct current-coated materials have smaller grain sizes and less plastic deformation compared with pulse current. The environmental conditions and the material type directly influence the surface topography and thus the friction coefficient and the wear resistance of the obtained coatings [16]. The material of the substrate results in changes in the adhesive strength of the deposited films. This varies with the different film/substrate combinations in the result of the crystallographic coherency between them. The eutectic and the peritectic alloy systems are practically applied in the electronic industry. The adhesion mechanism in the electronic device has attracted much attention. It depends on the number of voids that are observed in the mentioned interface and causes a decrease in the adhesion. The high concentration of the hydrogen existing in the elemental depth profiles results in the exfoliation of the film. Different interfacial structures were considered by Okamoto, Wang, and Watanabe [19] as well as Nweze and Ekpunobi [18] or Wei et al. In both articles, the substrate affects the crystal structure of the coatings and the crystallographic coherency itself. Additionally, the parameters of the electrodeposited layer are the function of the substrate thickness and its magnetic character [13, 14]. Gurrappa and Binder [11] showed an unbreakable link between specific free surface energy, adhesion energy, lattice orientation of the electrode surface, crystallographic lattice mismatch at the nucleus-substrate interface, and nanostructures of the electrodeposited coating. Its distribution depends on the nucleation and growth processes. The nucleation could be instantaneous or progressive. In the case of the first formation, the nuclei are increasing with time. During the progressive formation, nuclei gradually grow and overlap. The results of electrodeposition are strongly affected by the cathode surface and its characteristics. The growing near substrate layer filled up the holes and defects of the electrode surface. This yields the desired and oriented surface morphology on metallic or nonmetallic materials. In this case, surface engineering studies are very important to create a template (cathode surface) for specific applications [11, 32]. Some studies have shown a relationship between the refinement of the surface microstructure and the friction mechanical properties of the layers. Smoother surfaces give a lower friction coefficient [1, 2, 9]. Surface texturing i. e. generating a specific surface structure is one of the ways which can help with the reduction of the friction as well as surface coatings application or surface roughness improvement [25]. In the recent two decades, scientists developed the electrodeposition process beyond the current state of the art. Some of them (Fahidy, Aogaki) used the external magnetic field to extend the range of available properties in the context of magnetic, mechanical, or thermal applications of alloys and compounds. The others (Fritoceaux, Russo) changed the kind of substrate to check how it influences the properties of the coating/substrate system. All explorations have to give a response to the question of how the above act on the obtained coatings. Last three decades scientists reported that the applied external magnetic field (EMF, perpendicular, parallel) results in changes in the morphology and structure of the manufactured layers. Electrochemical reactions and magnetic field forces influence each other which causes the magnetohydrodynamic effect (MHD) creation. EMF induces the additional convection and reduces the diffusion layer (enhances mass transport). The conclusions of the research are as follows: i) parallel arrangement (II) of the field and electrode surface activates two-dimensional growth and smoother deposit; ii) perpendicular orientation (I_{\perp}) a rougher growth respectively. The field configurations (II, I_{\perp}) form the preferred crystal texture of the FeNi deposits [3, 36]. The use of electrochemical methods to modify the surface processes and materials modification itself are very important, especially when it comes to the needs of modern technologies. A lot of properties are exten-

sively investigated for this reason, including morphology, structural properties, hardness, corrosion, wear resistance, etc. Companies are intended in the development process of the nanostructured materials manufacturing which will play a significant role in their customer's market [11]. Nowadays, knowledge of the subject of magneto-electrodeposition plays a very important role in science and technology. An example could be the application in many industry branches like space research, military applications, security systems, high-density magnetic memories, navigation, medicine, etc. The aim of this paper was the experiments whose results allow the discussion about the morphological and crystallographic properties of the alloys deposited in the different physical conditions. What is new is looking for layers with properties that meet the needs of modern users. Currently, zinc can be found in the products of many industries and the economy. Among others, in medicine (bone repair material), in the automotive industry (anode in alkaline batteries). In many cases, Zn needs protection because it reacts with the surrounding environment (degradation, adhesion, corrosion resistance). For this reason, it is of interest to scientists from many research centers and still needs research to clarify many issues [27, 34].

2. Materials and methods

A direct current electrodeposition process was employed for the preparation of the FeNi layers. The platinum vertical plate (width-6 mm x height-5 mm x thickness-0,5 mm) was used as the anode, and electrochemically polished Cu and CuZn (Cu63Zn37 – manufacturer data) plates were used as the cathode (width-10 mm x height-20 mm x thickness-0,25 mm). The electrolyte for the preparation of the iron-nickel layer consisted of $\text{FeSO}_4 \cdot 7\text{H}_2\text{O}$ (7,5 g), $\text{NiSO}_4 \cdot 7\text{H}_2\text{O}$ (7,8 g), and H_3BO_3 (2 g) without the presence of additives. The whole process was performed galvanostatically using the potentiostat/galvanostat instrument (Matrix MPS-7163). The sets of two permanent magnets (width-75 mm x height-50 mm x thickness-10 mm) were placed in the especially designed laboratory stand around (parallel, perpendicular) the cathode surface. The magnetic field strength was measured with the gauge FH51 (Magnet-Physik) and ranged from 80 mT to 400 mT (with an accuracy of 2%) but near the electrode surface was distributed uniformly. The experiments were conducted at room temperature. Tribological analyses were carried out using a UMT TriboLab tribometer (Bruker, Billerica, MA, USA), with a ball-on-disc system under dry friction conditions and each of them took 300 s. The countersample was immobile 6 mm corundum ball. The reciprocating motion of a sample with the amplitude of 500 μm was repeated 3 times, with the following parameters: $F_n = 2 \text{ N}$, $f = 10 \text{ Hz}$. The knowledge about the composition was obtained as the result of spot surface measurement made with an energy dispersive X-ray spectrometer integrated with the SEM. X-ray diffractometer with Mo $K\alpha$ radiation ($\lambda = 0,713067 \text{ \AA}$) provided information on the crystal structure characterization. The probes were cut and the thickness of the cross-sections was measured. The LEXT OLS 4000 Confocal Laser Scanning Microscope (CLSM, Olympus, Tokyo, Japan) with a 3D image feature was used to characterize the metallic coatings: thickness, volume and depth of wear tracks. The often used method of surface description reflects the two other parameters. The first of them is the skewness (S_{sk}) which is sensitive to occasional deep valleys or high hills. It measures the symmetry of the variation of a profile about its mean line and gives information about the number of hills or valleys on the surface. Zero skewness informed about symmetrical height distribution. Positive value testifies to the fact of the existence of fairly high spikes above a flatter average. A negative value describes filled valleys, and deep scratches in a smoother plateau. The second is the kurtosis (S_{ku}), which informs about the probability density sharpness of the profile. An increase in the S_{sk} value results in an increasing trend in the value of the friction static coefficient. In the case of S_{ku} , we observe the opposite trend. Positive S_{sk} shows surfaces with good adhesion resistance but negative leads to lower values [25]. Both mentioned variables should be

calculated to achieve a useful understanding of a composite surface [1, 2, 20, 25, 26, 29]. Roughness of the probes was measured with the use of the optical method (not as a classic linear profilometer) but it was shown as a section of the surface with marked roughness values. Microhardness was tested using the Vickers method with a load of 0,9807 N and repeated 10 times. The crystal sizes were calculated by the use of Powder Cell program which adapts experimental (powder diffraction patterns) and theoretical data automatically.

3. Results and Discussion

3.1. X-Ray Diffraction (XRD)

The crystalline structures of the alloys deposited on both substrates (Cu, CuZn) show a dependence in respect of the deposition time (Fig.1). After 900 s of the process, the FeNi coatings are dominated by the FeNi structure. Long-term deposition causes a mixture of FeNi and Fe phases with the primary occurrence of bcc-Fe which confirms the data presented in Fig.3 (showing the changes in the Fe content). The addition of zinc (37 %) to Cu, as it is in the brass substrate changes the crystal cells parameters by 2 percent (value of the crystal parameter). For Cu, c is equal to 3,57 Å and for CuZn – 3,65 Å which are close to the theoretical values of $c = 3,581$ Å in FeNi (JCPDS Card No. 47-1405) and $c = 3,647$ Å in Fe (JCPDS Card No. 06-0696) respectively [21, 22]. The external magnetic field application influences the crystallites size. In both cases (Cu and CuZn) crystallites are larger when growing without EMF. In average respectively $d=23,0 \pm 1,0$ nm in comparison of the EMF presence $d=14,0 \pm 1,0$ nm (FeNi crystallites - Cu substrate and Fe - CuZn). Therefore EMF works as the grain refiner.

3.2. Scanning Electron Microscopy (SEM)

Fig.2 shows the morphology of the fabricated FeNi coatings which changes due to the presence and the orientation of the EMF obtained by scanning electron microscopy. The surface of the de-

posit becomes smooth and compact when no external magnetic field was applied. Resulted layers seem to grow following a progressive nucleation mechanism. The presence of the external magnetic field during the deposition process doesn't influence the nucleation mechanism itself but affects the subsequent growth of the objects. In this case (at the early stage of the deposition, 900 s), it leads to a preferential development of 3D forms into clusters on the 2D nucleation centers at fixed points (deterministic mode). Over the time (3600 s), the number of these places increases, and 3D growth centers are scattered over almost the entire surface at various stages of development and various sizes (stochastic mode). The coating on both substrates (Cu, CuZn) showed competitive growth of 2D and 3D forms.

The major effect of the magnetic field is known as the magneto-hydrodynamic (MHD) effect which results in additional convection and therefore reduction of the diffusion layer thickness. This caused the enhanced mass transport to the existing deposit and increased

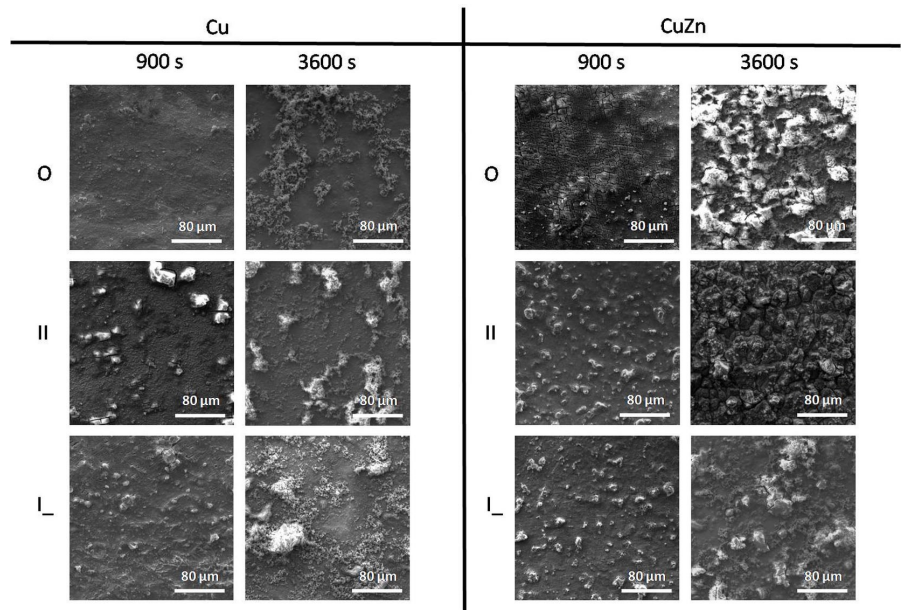


Fig.2. Set of SEM images of the deposited films with and without EMF: different time deposition (900, 3600 s); different substrate (Cu, CuZn); current density – 50 mA (cm²)⁻¹; without EMF (A), II EMF (B), I - EMF (C)

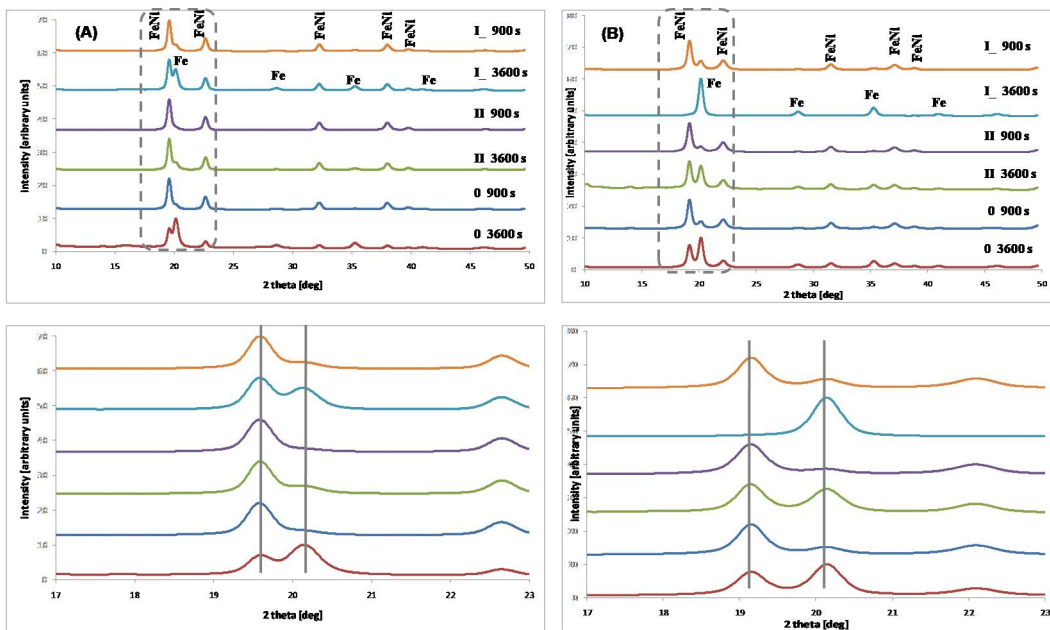


Fig.1. Selected XRD patterns are presented in panels concerning substrate surface: copper (A), brass (B), and time (900 s, 3600 s), respectively (0 – without EMF, II – parallel EMF, I – perpendicular EMF); current 50 mA (cm²)⁻¹

the secondary nodules (second micro-MHD effect) [17]. This growth type appears as the result of instantaneous nucleation which characterizes a slow growth of the nuclei with a quite small number of active sites at the same moment [4]. Only the layer on CuZn substrate after II EMF application characterizes cracks and nodular shapes of the growing layer. This is directly connected with the appearance of high content of Ni (decrease of Fe content in time – Fig.3) and the increase of the hydrogen evolution rate [35]. This results in the grooves (among 3D nuclei) indented by MHD-flow and the hydrogen formation (reaction between Ni in alloy and Zn from the substrate) [17, 35].

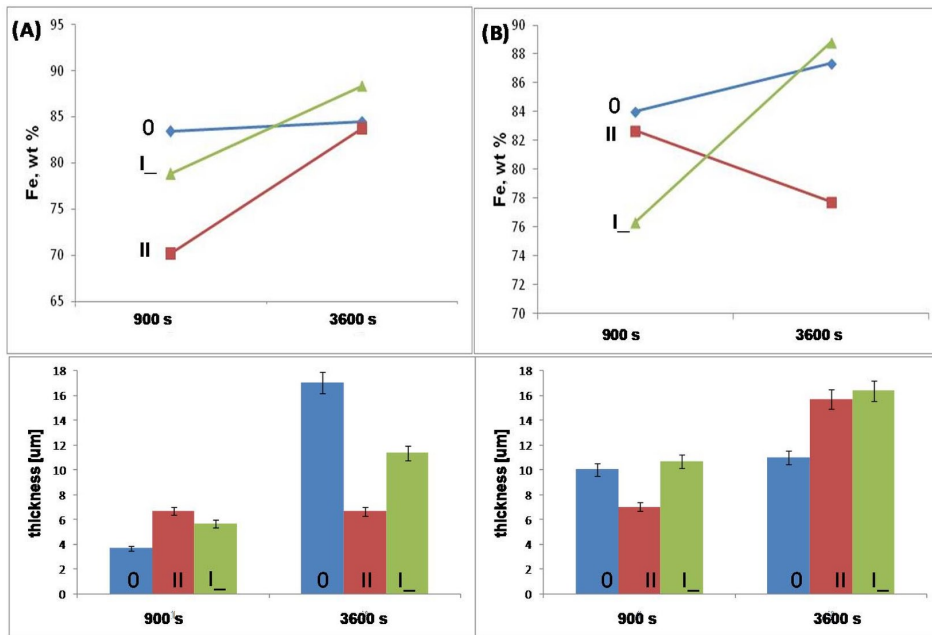


Fig. 3. Effect of Fe content (upper row) and FeNi film thickness (lower row) in time; (A) Cu substrate, (B) CuZn substrate; 0 – without EMF, II – parallel EMF, I_ – perpendicular EMF

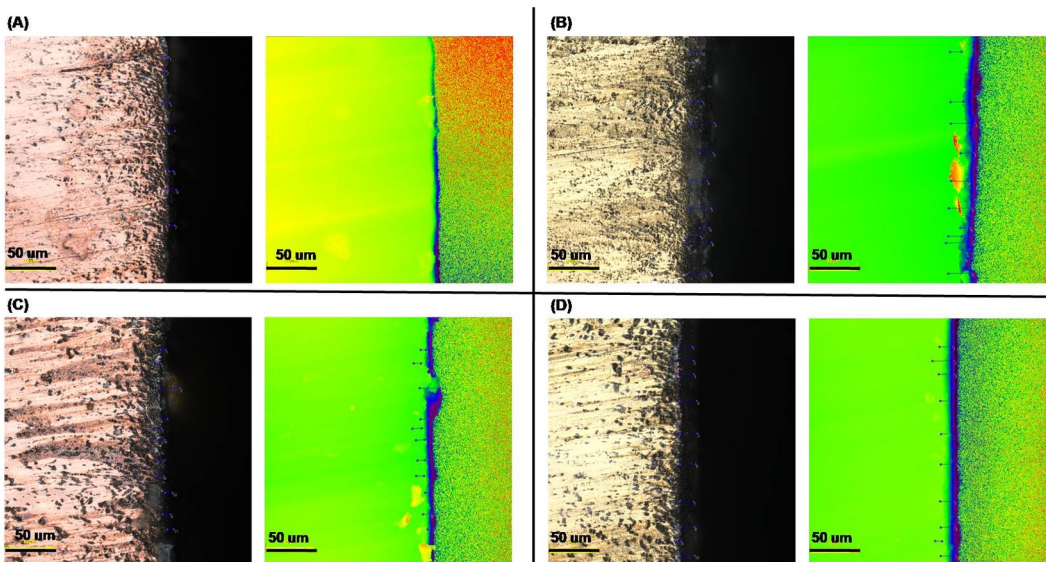


Fig. 4. Set of SEM images of the deposited films cross-sections without (A, B) and with II EMF (C, D): time deposition 900 s; different substrate – Cu (A, C), CuZn (B, D); current density – $50 \text{ mA (cm}^2\text{)}^{-1}$

As the result of the electrodeposition process composition gradients in FeNi coatings occurred. The experiments clarified the dependence of the thickness and time for the elemental composition of the coatings. Fig.3A shows the upward trend of the iron amount in all cases (without and with the presence of the EMF) with the time increasing. It is defined as an anomalous co-deposition, where the iron (less noble metal) percentage in the deposit is higher than its presence in the electrolyte (Fe:Ni – 1:1), especially with the longer time of deposition (Brenner, Tabakovic) [1]. The EMF application (at the later stage of deposition) reduces the thickness of the layer on a copper substrate compared to a deposition without an external magnetic field during the longer time of process duration (Fig.4). This is the result of the MHD effect which was mentioned earlier. The case of deposition on CuZn substrate (Fig.3B) differs from mentioned above Cu substrate. The iron content decreases after a longer time of the II EMF application as reflected in the sediment morphology (Fig.2 – CuZn, 3600 s, II EMF). The presence of EMF enlarges the thickness of the deposit. In the case of Cu substrate, it is visible especially in the early stages of

electrodeposition (Fig.3A), but in the case of CuZn substrate (Fig.3B), this situation appears after a long time of electrodeposition process duration. It is inherently related to the increase in roughness of the deposited FeNi coatings in the above-discussed cases (Fig.5 and 6) due to enhanced mass transport (MHD effect) of the refined grains.

3.3. Tribological tests

First, the roughness of the substrates was measured. As a result, the values of skewness and kurtosis were obtained. For Cu substrate: 0,11 and 4,55 and CuZn: -0,66 and 4,82 respectively.

Positive values of the S_{sk} parameter inform about the predominance of peaks on the measured surfaces (Fig.7.). The surfaces have irregularities, the rough surface becomes spiky and a large number of hills are in contact. The higher values of positive skewness result in good adhesion force and resistance under a certain load which characterizes obtained FeNi coating. A lot of asperities increase the real area of contact [30]. This is especially visible in the cases of EMF absence (Cu substrate) and perpendicular EMF (CuZn substrate) for 900 s deposition time duration, when the values of S_{sk} are the highest –11,08 and 11,88 (Fig.7). In the same cases, values of $S_{ku} > 3$ (17,04 and 18,50) reveal the presence of larger grains in the profile of the surface – 20,00 nm (Cu substrate) and 17,00 nm (CuZn substrate) [7, 10, 36].

Due to the dynamic nature of changes in friction conditions, low reproducibility is very common in tribological tests. These changes can be caused by the lapping of kinematic pairs surfaces and generating wear products, often in a stochastic way. These products can be removed beyond the friction zone

or remain inside and intensify the secondary wear. The high dynamic of changes in the tribological system has a significant impact on the resistance to motion of the kinematic pair, which analysis is usually used to determine the frictional characteristics of the material. Despite this, friction tests allow to observe some tendencies and dependencies. Results of the wear tests were summarized in Fig.8 and 9.

At high kurtosis values, the asperities become much peakier which drastically decreases the effect of the friction force. Therefore, the coefficient of friction increases slightly to reach the greatest value and decreases further (Fig.8 and 9) [30]. The roughness has the lowest values in both mentioned cases. There are consequences of the appearance of fragments of the damaged surfaces and debris rather than the sharp edges of the deposited FeNi layer [6, 15, 26]. In the case of Cu substrate, the surface characterizes the predominance of peaks but CuZn – of valleys. Roughness profiles of the substrates influence the layers growth to a small extent.

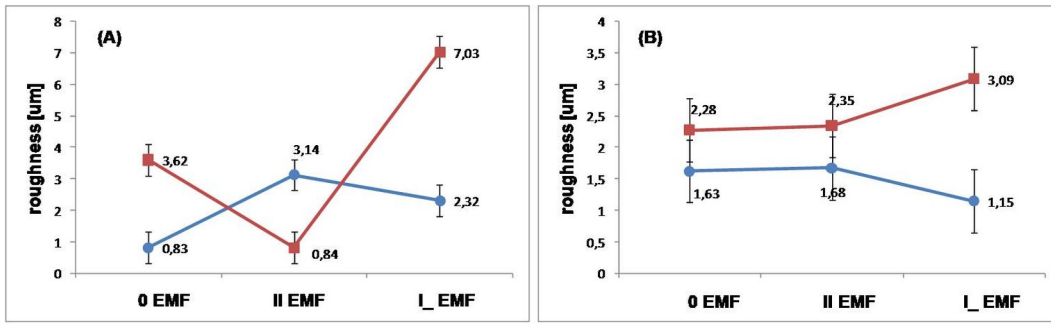


Fig. 5. Values of the roughness of tested surfaces: Cu substrate (A), CuZn substrate (B); time: 900 s – blue line (points), 3600 s – red line (square)

The resistance to motion analysis shows that they are highly dependent on the type of the substrate and the deposition time of the FeNi coating. An intensive rise and subsequent sharp decline in the value of the friction coefficient often occurs in the initial stage of wear ($S_{ku} > 5$). It is related to abrasion of surface irregularities, and it can be observed especially for CuZn substrates with a 900 s layer deposition time. The stage of gradual lapping of the surface layer is associated with the lack of rapid changes in the value of the coefficient of friction. As the substrate was exposed, the resistance to the motion increased (Fig. 8 and 9). It particularly occurred for Cu substrates.

The results of the wear track morphology studies presented in Fig.10 showed that in most cases the depth of friction marks increased with the thickness of the layer. Although the thicker FeNi coatings were significantly worn, in most cases their breakthrough was not observed. The opposite tendency can be seen for the layers with a shorter deposition time, where the substrate was fully (Cu) or partially (CuZn) exposed due to friction. Thus, it seems that the coatings on CuZn substrates show higher wear resistance. It is related to an increased degree of adhesion of the layer to the substrate which is in connection with the highest values of skewness and kurtosis - Fig.7 [23,

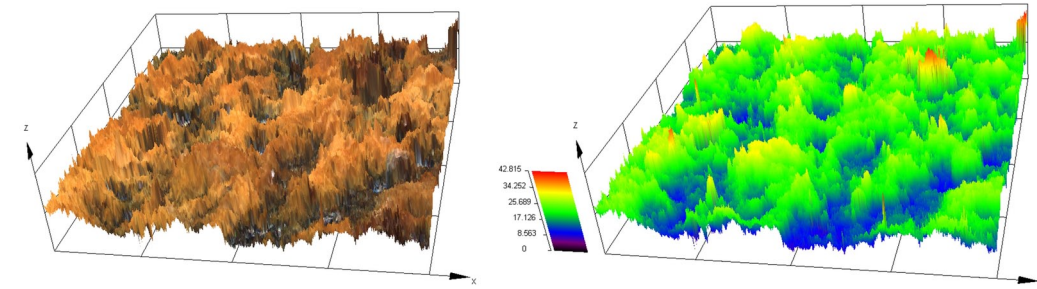


Fig. 6. Set of images of the surface roughness of the deposited films, Cu substrate, 3600 s, without EMF

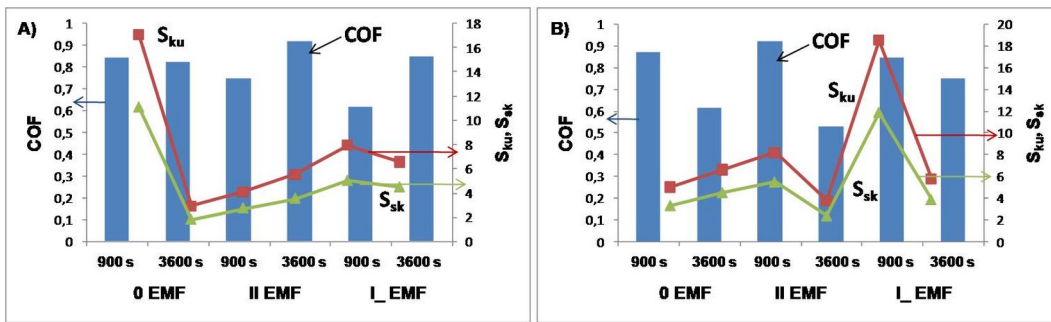


Fig. 7. Values of the friction coefficient after 300 s of the process (COF, blue box), the kurtosis - S_{ku} (red, square), and the skewness - S_{sk} (green, triangle) for coated samples of Cu substrate (A) and CuZn substrate (B)

26, 30]. After the layers deposition, the samples were not rinsed in the ultrasonic cleaner due to the possibility of the layer chipping. They were rinsed only with distilled water. During the tribological tests, the wear products (substrate particles - Cu, Zn, and their oxides) produced a mixture, so it may seem that the trace after friction is shallower (Fig.8, 9 and 10).

On the other hand, SEM images presented in Fig.11 show that thicker coatings may crack and chip. This generates wear products, which are placed in the friction zone. The brittleness of coatings formed at 3600 s deposition time is associated with their decreased microhardness (Fig.12). Due to the movement of the kinematic pair, wear products are crushed and shredded. Thermal energy from friction can lead to their oxidation and formation of oxides. A large amount of wear debris intensifies wear. The microscopic analysis shows that the dominant type of wear was three-body abrasion. Overtime, when the substrate was

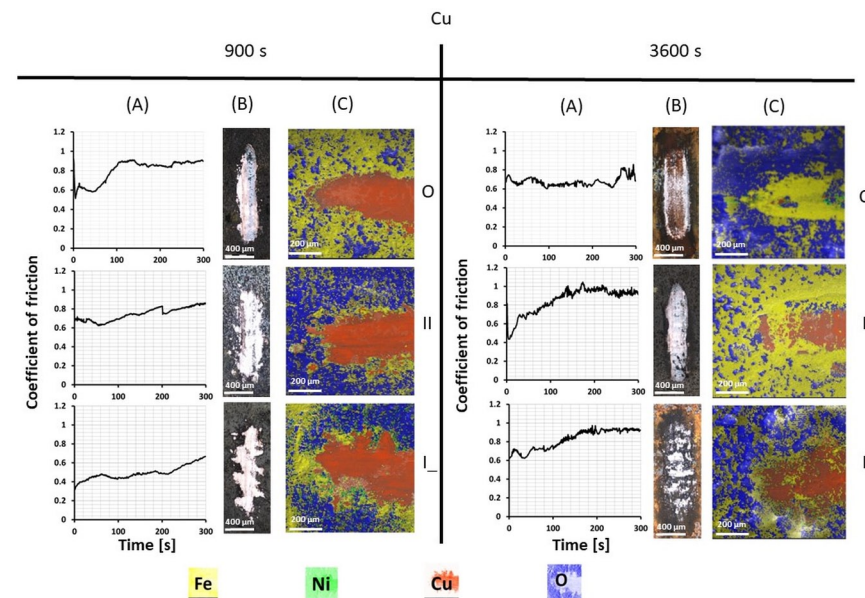


Fig. 8. Results of tribological tests for Cu substrate for different times of layer deposition 900 s and 3600 s (0 – without EMF, II – parallel EMF, I – perpendicular EMF): coefficient of friction vs. time (A), CLSM images of friction marks (B), SEM-EDX analysis of wear tracks (C)

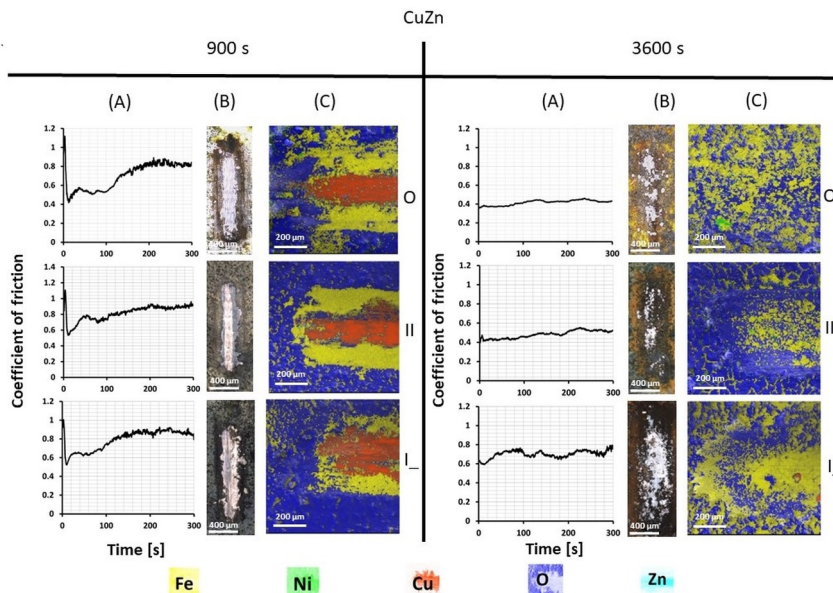


Fig. 9. Results of tribological tests for CuZn substrate for different times of layer deposition 900 s and 3600 s (0 – without EMF, II – parallel EMF, I – perpendicular EMF): diagrams of coefficient of friction vs. time (A), CLSM images of friction marks (B), SEM-EDX analysis of wear tracks (C)

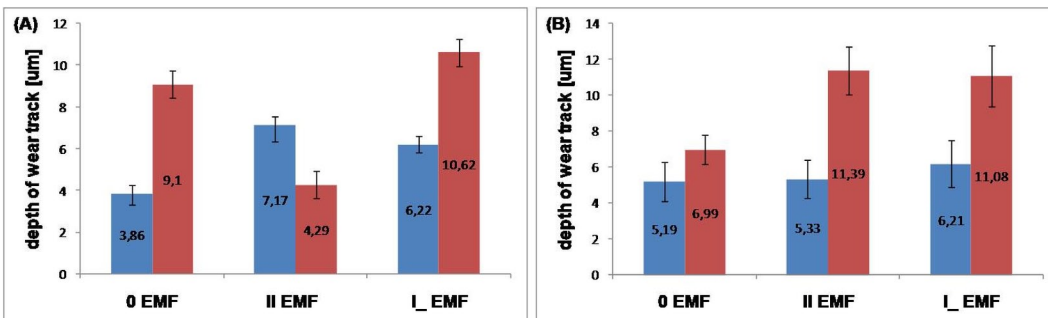


Fig. 10. Depth of the friction marks for FeNi coating on: Cu substrate (A) and CuZn substrate (B); $F_N=2\text{ N}$, $f=10\text{ Hz}$; 900 s – left columns (blue), 3600 s – right columns (red)

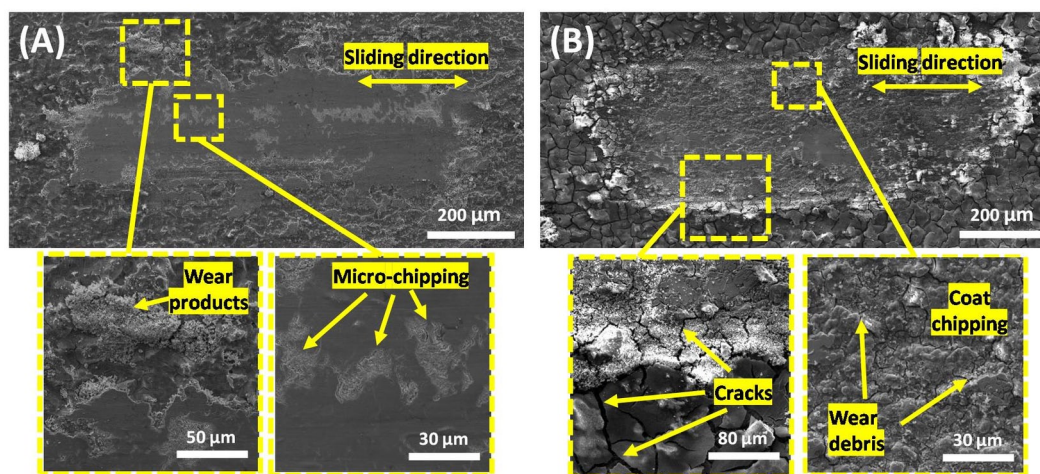


Fig. 11. Set of SEM photos of wear tracks for Cu substrate, 900 s of II EMF (A); CuZn substrate, 3600 s of II EMF (B)

exposed to the motion, the amount of generated wear particles decreased, and the surface was smoothed out [38].

Increasing the Fe content (Fig.3) while extending the time of deposition is correlated with higher values of the microhardness (Fig.12). Except in the case of the film deposition on the CuZn substrate in the presence of II EMF when the dependence is opposite, the Fe content and the value of the microhardness decrease. This scenario confirms

also XRD analysis (Fig.1) then the peaks typical for metallic Fe appear and are much more intensive.

In most of the considered cases, the intensity of friction marks and values of microhardness (Fig.12) increased with the deposition time except for II EMF on CuZn substrate. The aforementioned dependence is also influenced by the composition of the FeNi coating, as the result, the high content of the iron oxides causes deeper friction marks (Fig.8, 9, and 10). Higher values of the microhardness are connected with the Fe content increase which was shown in Fig.3. The opposite relationship of microhardness in the case of II EMF on CuZn substrate is in agreement with a decrease in Fe content. This is due to the observation that the thickness of the layer was increasing till the end of the experiment. X-ray analysis of the elemental composition of the obtained layers subjected to friction process confirms the increased wear resistance connected with raised Fe content in both scenarios with the absence and presence of the external magnetic field [34].

4. Conclusion

The experimental investigation suggests that the electrodeposition process can be modified by applying various orientations of the external magnetic field. The type of layer growth changes from progressive to instantaneous. This may be attributed to the effect caused by mass transfer induced in the electrolytic solution (MHD effect). Extending the duration of the process itself also affects the mode of growth. The early stages of deposition are assigned as a deterministic mode and later – a stochastic one. The surface morphology of the coatings is related to the Fe content and type of the substrate. Further, certain changes in the coefficient of friction are due to an increase in the kurtosis value. Higher wear resistance, as well as coatings adhesion to the substrate, are depending on the higher value of skewness. The increase in microhardness is attributed to the favorable iron electrodeposition which was supported by the XRD study [32]. These findings are of practical significance since they can aid engineers in selecting appropriate surface roughness/textures based on their specific requirements [30].

Undoubtedly, the external magnetic field used during the deposition allows for the fragmentation of the FeNi coatings, thus obtaining better tribological properties. It is a starting point for further research on the wettability of such surfaces and the durability of layers in nanoelectronics.

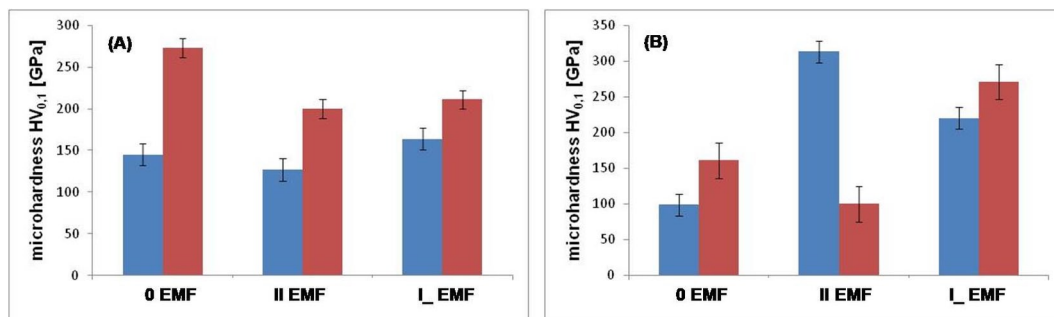


Fig. 12. Values of microhardness of tested surfaces: Cu substrate (A), CuZn substrate (B); deposition time: 900 s – left columns (blue), 3600 s – right columns (red)

Acknowledgments

This work was partially financed by the EU fund as part of the projects: POPW.01.03.00-20.034/09 and POPW.01.03.00-20-004/11, and WZ/WE-IA/2/2020 supported by a research subsidy of the Institute of Automation, Electronics and Electrotechnology Bialystok University of Technology for 2022, assigned as teamwork. This research was realized in the frame of work No. WZ/WM-IIB/2/2020 and partially financed from research funds of the Ministry of Education and Science Poland.

References

- Białostocka A, Idzkowski A. The effect of Ground Changes and the Setting of External Magnetic Field on Electroplating FeNi Layers: Progress in Automation, Robotics and Measurement Techniques in Automation 2019;684-696.
- Białostocka AM, Klekotka U, Kalska-Szostko B. The Influence of the Substrate and External Magnetic Field Orientation on FeNi Film Growth. Energies 2022; 15 (10): 1-12. <https://dx.doi.org/10.3390/en15103520>.
- Chen L, Liu Z, Wang X, et al. Effects of Surface Roughness Parameters on Tribological Performance for Micro-textured Eutectic Aluminum–Silicon Alloy. Journal of Tribology 2020; 142 (2): 021702, <http://dx.doi.org/10.1115/1.4044990>.
- Daltin AL, Benaissa M, Chopart JP. Nucleation and crystal growth in magneto-electrodeposition. Materials Science and Engineering 2018; 424: 012022, <http://dx.doi.org/10.1088/1757-899X/424/1/012022>.
- Dragos O, Chiriac H, Lupu N, et al. Anomalous Codeposition of fcc NiFe Nanowires with 5-55 % Fe and Their Morphology, Crystal Structure and Magnetic Properties. Journal of The Electrochemical Society 2016;163(3): D83-D94, <http://dx.doi.org/10.1149/2.0771603jes>.
- Duboust N, Ghadbeigi H, Pinna C, et al. An optical method for measuring surface roughness of machined carbon fibre-reinforced plastic composites. Journal of Composite Materials 2017; 51(3): 289-302, <http://dx.doi.org/10.1177/0021998316644849>.
- Dzierwa A, Gałda L, Tupaj M, et al. Investigation of wear resistance of selected materials after slide burnishing process. Eksploatacja i Niezawodność – Maintenance and Reliability 2020;22 (3): 432-439, <http://dx.doi.org/10.17531/ein.2020.3.5>.
- Dziurka R, Madej M, Kopyściński M, et al. The influence of microstructure of medium carbon heat-treatable steel on its tribological properties. Key Engineering Materials 2015;641: 132-135, <http://dx.doi.org/10.4028/www.scientific.net/KEM.641.132>.
- Góral A, Lityńska-Dobrzyńska L, Kot M. Effect of Surface Roughness and Structure Features on Tribological Properties of Electrodeposited Nanocrystalline Ni and Ni/Al₂O₃ Coatings. Journal of Materials Engineering and Performance 2017; 26(5): 2118-2128, <http://dx.doi.org/10.1007/s11665-017-2662-2>.
- Grzesik W, Niesłony P, Habrat W. Investigation of the tribological performance of AlTiN coated cutting tools in the machining of Ti6Al4V titanium alloy in terms of demanded tool life. Eksploatacja i Niezawodność – Maintenance and Reliability 2019; 21 (1): 153-158, <http://dx.doi.org/10.17531/ein.2019.1.17>.
- Gurrappa I, Binder L. Electrodeposition of nanostructured coatings and their characterization – A review. Science and Technology of Advanced Materials 2008;9: 043001 (11 pp), <http://dx.doi.org/10.1088/1468-6996/9/043001>.
- Gül H, Uysal M, Akbulut H, et al. Tribological Behavior of Copper/MWCNT Nanocomposites Produced by Pulse Electrodeposition. Acta Physica Polonica A 2014;125: 254-256, <http://dx.doi.org/10.12693/APhysPolA.125.254>.
- Khazi I, Mescheder U. Micromechanical Properties of Anomalous Electrodeposited Nanocrystalline Nickel-Cobalt Alloys: A Review. Materials Research Express 2019, <http://dx.doi.org/10.1088/2053-159/ab1bb0>.
- Kuru H, Kockar H, Alper M. Giant magnetoresistance (GMR) behavior of electrodeposited NiFe/Cu multilayers: Dependence of non-magnetic and magnetic layer thickness. Journal of Magnetism and Magnetic Materials 2017;444: 132-139, <http://dx.doi.org/10.1016/j.jmmm.2017.08.019>.
- Macek W, Szala M, Trembacz J, et al. Effect of non-zero stress bending-torsion fatigue on fracture surface parameters of 34CrNiMo6 steel notched bars. Production Engineering Archives 2020; 26(4): 167-173, <http://dx.doi.org/10.30657/pea.2020.26.30>.
- Mbugua NS, Kang M, Zhang Y, et al. Electrochemical Deposition of Ni, NiCo Alloy and NiCo-Ceramic Composite Coatings – A Critical Review. Materials 2020;13: 3475, <http://dx.doi.org/10.3390/ma13163475>.
- Morimoto R, Miura M, Sugiyama A, et al. Long-Term Electrodeposition under a Uniform Parallel Magnetic Field. 1. Instability of Two-Dimensional Nucleation in an Electric Double Layer. The Journal of Physical Chemistry 2020; 124; 52: 11854-11869, <http://dx.doi.org/10.1021/acs.jpcc.0c05903>.
- Nweze CI, Ekpunobi AJ. Electrodeposition of Zinc Selenide Films on Different Substrates and Its Characterization. International Journal of Scientific & Technology Research 2014; 3; 9.
- Okamoto N, Wang F, Watanabe T. Adhesion of Electrodeposited Copper, Nickel and Silver Films on Copper, Nickel and Silver Substrates. Materials Transactions 2004; 45; 12: 3330-3333.
- Palomar-Pardavé M, Scharifker BR, Arce EM, et al. Electrochimica Acta 2005; 50: 4736-4745, <http://dx.doi.org/10.1016/j.electacta.2005.03.004>.
- Persson K. Materials Data on FeNi (SG:123) by Materials Project. 10.17188/1197364 (2016).

22. Persson K. Materials Data on FeNi₃ (SG:221) by Materials Project. 10.17188/1190197 (2015).
23. Rao VR, Bangera KV, Hegde ACh. Magnetically induced electrodeposition of Zn-Ni alloy coatings and their corrosion behaviors. *Journal of Magnetism and Magnetic Materials* 2013; 345: 48-54, <http://dx.doi.org/10.1016/j.jmmm.2013.06.014>.
24. Rezende GLT, Cesar VD, do Lago CBD, et al. A review of Corrosion Resistance Nanocomposite Coatings. *Electrodeposition of Composite Materials*; 147-185, <http://dx.doi.org/10.5772/62048>.
25. Sedlaček M, Gregorčič P, Podgornik B. Use of the roughness parameters S_{sk} and S_{ku} to control friction – a method for designing surface texturing. *Tribology Transactions* 2016, <http://dx.doi.org/10.1080/10402004.2016.1159358>.
26. Sedlaček M, Podgornik B, Vižintin J. Correlation between standard roughness parameters skewness and kurtosis and tribological behaviour of contact surfaces. *Tribology International* 2012; 48: 102-112, <http://dx.doi.org/10.1016/j.triboint.2011.11.008>.
27. Shuai C, et al. A peritectic phase refines the microstructure and enhances Zn implants. *Journal of Materials Research and Technology* 2020; 9(3): 2623-2634, <https://dx.doi.org/10.1016/j.jmrt.2020.04.037>.
28. Sriraman KR, Manimunda P, Chromik RR, et al. Effect of crystallographic orientation on the tribological behavior of electrodeposited Zn coatings. *Communication* 2016;6: 17360, <http://dx.doi.org/10.1039/c5ra15490a>.
29. Svahn F, Kassman-Rudolphi Å, Wallén E. The influence of surface roughness on friction and wear of machine element coatings. *Wear* 2003; 254: 1092-1098, [http://dx.doi.org/10.1016/S0043-1648\(03\)00341-7](http://dx.doi.org/10.1016/S0043-1648(03)00341-7).
30. Tayebi N, Polycarpou AA. Modeling the effect of skewness and kurtosis on the static friction coefficient of rough surfaces. *Tribology International* 2004; 37: 491-505, <http://dx.doi.org/10.1016/j.triboint.2003.11.010>.
31. Thomas BG. *Metals Processing. Structure, Processing, and Properties of Engineering Materials*. editor J. Adams, Wesley A., chapter 14.
32. Torabinejad V, Aliofkahaerai M, Rouhaghdam SA, et al. Tribological behavior of electrodeposited Ni-Fe multilayer coating. *Tribological Transactions* 2016, <http://dx.doi.org/10.1080/10402004.2016.1230687>.
33. Tudela I, Zhang Y, Pal M, et al. Ultrasound-assisted electrodeposition of nickel: Effect of ultrasonic power on the characteristics of thin coatings. *Surface & Coatings Technology* 2015; 264: 49-59, <http://dx.doi.org/10.1016/j.surfcoat.2015.01.020>.
34. Wang Z-B, Li W-Y, Shang S, et al. Performance degradation comparisons and failure mechanism of silver metal oxide contact materials in relays application by simulation. *Eksploatacja i Niezawodność – Maintenance and Reliability* 2020; 22 (1): 86-93, <http://dx.doi.org/10.17531/ein.2020.1.10>.
35. Wei X, et al. Impact of anode substrates on electrodeposited zinc over cycling in zinc-anode rechargeable alkaline batteries. *Electrochimica Acta* 2016; 212: 603-613, <https://dx.doi.org/10.1016/j.electacta.2016.07.041>.
36. Yang L-L, Chen ChCh, Yuan J, et al. Effect of applied magnetic field on the electroplating and magnetic properties of amorphous FeNiPGd thin film. *Journal of Magnetism and Magnetic Materials* 2020; 495: 165872, <https://dx.doi.org/10.1016/j.jmmm.2019.165872>.
37. Zangari G. *Electrodeposition of Alloys and Compounds in the Era of Microelectronics and Energy Conversation Technology*. *Coatings* 2015: 195-218, <http://dx.doi.org/10.3390/coatings5020195>.
38. Żurowski W. Structural factors contributing to increased wear resistance of steel friction couples. *Eksploatacja i Niezawodność – Maintenance and Reliability* 2012; 14 (1): 19-24.